ELSEVIER

Catalysis Today 48 (1999) 31–40

CATALYSIS TODAY

Vapor-phase kinetics and its contribution to global three-phase reaction rate in hydrogenation of 1-methylnaphthalene

Shinya Ishigaki[a,*], Shigeo Goto[b]

[a]*Kinuura Research Center, JGC Corporation, 2-110 Sunosaki-cho, Hande, Aich 475-0021, Japan*
[b]*Department of Chemical Engineering, Nagoya University, Chikusa, Nagoya 464-8603, Japan*

Abstract

It has been considered that the contribution of the vapor-phase reaction (VPR) to the global three-phase reaction rate may become much lower as the catalyst effectiveness factor approaches unity. In this study, the hydrogenation of 1-methylnaphthalene was performed as an example of slow reactions using a laboratory-scale trickle-bed reactor (TBR) at 583 K, 8.0 MPa. It was qualitatively confirmed that VPR contributed to the product yields in TBR even in this slow reaction system when the liquid velocity was low and the volatility of the liquid was high. Langmuir–Hinshelwood type kinetic equations were established for the vapor-phase reaction. The product yields in TBR neither be explained by liquid- vapor-phase kinetics without external effects, nor the conventional partial wetting model. Therefore, a partial wetting model considering the contribution of VPR was proposed where the catalyst bed composed of externally partial and internally complete wet particles, and completely dry particles was assumed. Using this model, the product yields in TBR were suitably explained.

Keywords: Trickle-bed reactors; Partial wetting; Hydrogenation; 1-Methylnaphthalene; Kinetics

1. Introduction

The global reaction rate in the gas–liquid–solid three-phase reaction ($r'_{GL,j}$) has been usually analyzed by two types of partial wetting models.

One model assumes that the internal volume of porous catalyst is completely filled with liquid due to capillary forces [1]. In this model, the reaction catalyzed in the liquid-phase which proceeds at a rate of $r'_{L,j}$ only affects the global reaction rate. The global reaction rate can be approximated by the sum of contributions from wetted and non-wetted external surfaces using the wetting efficiency of catalyst (f_w) as a weighting factor [2]:

$$r'_{GL,j} = f_w r'_{L,j}(C_L) + (1 - f_w) r'_{L,j}(C_L^*). \quad (1)$$

The second term in Eq. (1) corresponds to the reaction rate in the non-wetted external surface where the surface concentrations can usually approach those in the vapor–liquid equilibrium (C_L^*) because the gas-to-solid mass transfer resistances can be assumed to be negligibly small.

The other partial wetting model assumes the presence of the dry part of catalyst particle where the vapor-phase reaction (abbreviated as VPR) proceeds at a rate of $r'_{G,j}$ and affects the global reaction rate. The dry part may appear as a result of the vaporization of volatile liquid components induced by poor heat

*Corresponding author.

0920-5861/99/$ – see front matter
PII: S0920-5861(98)00355-1

transfer at the gas–solid interface in highly exothermic reactions. Satterfield and Ozel [3] presented experimental evidence to show that VPR took place in hydrogenation of benzene at 349 K and atmospheric pressure. Sedriks and Kenney [4], in the selective hydrogenation of crotonaldehyde at 304 K and atmospheric pressure, found that VPR was considerable at a low liquid superficial velocity (4.5×10^{-5} m/s) and explained their experimental results using the following simple expression of the global reaction rate by considering the contribution of VPR:

$$r'_{GL,j} = f_w r'_{L,j}(C_L) + (1 - f_w) r'_{G,j}(C_G). \quad (2)$$

This equation has been adopted to determine f_w in the hydrogenation of naphthalene at high temperature and pressure (513 K and 5.17 MPa) by Huang and Kang [5]. The catalyst effectiveness factors in the reactions performed by these three research groups were very low. In such a case, VPR proceeding in the thin dry layer around the catalyst particle can greatly influence to the global reaction rate while the inside of the catalyst is filled mostly with liquid.

It has been considered that the contribution of the VPR to the global reaction rate may become much lower as the catalyst effectiveness factor approaches unity [4]. However, the contribution of VPR in a slow reaction has been suggested by Ruecker and Akgerman [6] in the hydrogenation of biphenyl at 566 K and 5.2 MPa. In our previous studies on the hydrogenation of biphenyl at 566 K and 5.2 MPa. In our previous studies on the hydrogenation of 1-methylnaphthalene [7,8] where the catalyst effectiveness factor was greater than 0.6 [9], the contribution of VPR was also suggested from the comparison of three-phase kinetic measurements between an improved stirred basket-type batch reactor and a coiled tubular flow-type reactor.

The purposes of this study are

1. to investigate when the VPR is considerable in a slow reaction, and
2. to explain quantitatively the contribution of VPR to the global reaction rate by the modification of conventional partial wetting models.

The hydrogenation of 1-methylnaphthalene was performed as an example of slow reactions using a laboratory-scale trickle-bed reactor operated at high temperature and pressure, and low liquid flow rates where the liquid-phase was highly volatile.

2. Experimental

2.1. Catalyst

The catalyst used was a commercially supplied Co–Mo/γ-Al_2O_3 catalyst (CDS-D21, manufactured by Catalyst and Chemicals Ind., Japan) with a cylindrical shape of 1.6 mm diameter and 4.0 mm length. The catalyst contained 4.3 wt% CoO and 17.1 wt% MoO_3. Powdered catalyst of 0.1 mm average diameter was also prepared by powdering this catalyst to obtain intrinsic kinetic data in the vapor-phase. These catalysts were presulfided with a mixture of 3 mol% hydrogen sulfide and 97 mol% hydrogen at 603 K temperature and 1000 h^{-1} gas hourly space velocity, for 12 h under atmospheric pressure.

2.2. Feed liquid for the three-phase reaction

Feed liquid used for the three-phase reaction contained 10 wt% 1-methylnaphthalene (1-MN) and a mixture of normal paraffins as solvent (named NPL consisting of 62.4 wt% *n*-tetradecane, 29.7 wt%, *n*-pentadecane 6.7 wt% *n*-hexadecane and 1.2 wt% *n*-heptadecane). Carbon disulfide was added into the feed liquid to a level of 0.3 wt% to maintain the catalyst in the sulfied form during the reaction.

2.3. Feed gas for the vapor-phase reaction

The vapor-phase reaction was performed with hydrogen and a vaporized mixture of 10 wt% 1-MN, 0.3 wt% carbon disulfide and a solvent. Normal heptane was selected for the solvent to investigate the vapor-phase kinetics for the truly dry catalyst. The composition of feed gas was changed as shown in Table 1 (named Feed-A, -B and -C) to examine the effect of partial pressures of 1-MN and hydrogen.

Table 1
Feed gas compositions for vapor-phase hydrogenation of 1-MN (mol%)

	Feed-A	Feed-B	Feed-C
Hydrogen	91.34	94.06	96.35
1-MN	1.23	0.84	0.52
n-Heptane	7.43	5.10	3.13

2.4. Apparatus and procedure

2.4.1. Three-phase reaction using a trickle-bed reactor

The three-phase reaction was performed using a trickle-bed reactor (TBR). Fig. 1 shows a schematic drawing of TBR system. The reactor (A) was a stainless steel tube of 27.2 mm inner diameter and 1.55 m length, equipped with a liquid preheater ((C) 16.1 mm inner diameter and 1.0 m height packed with inert alumina balls of 1 mm diameter), an inlet liquid distributor (D) and a product flash separator ((G) abbreviated as PFS) placed at the outlet of catalyst bed (B). The reactor was placed in a fluidized sand bath heater.

The feed liquid was fed to the top of a mixing bed ((F) 1.0 m height packed with inert alumina balls of 1 mm diameter) through 13 capillary tubes of 0.5 mm inside diameter where the liquid contacted hydrogen. In the mixing bed, the liquid feed can sufficiently contact hydrogen. Hence, we can assume the vapor–liquid equilibrium at the inlet of catalyst bed.

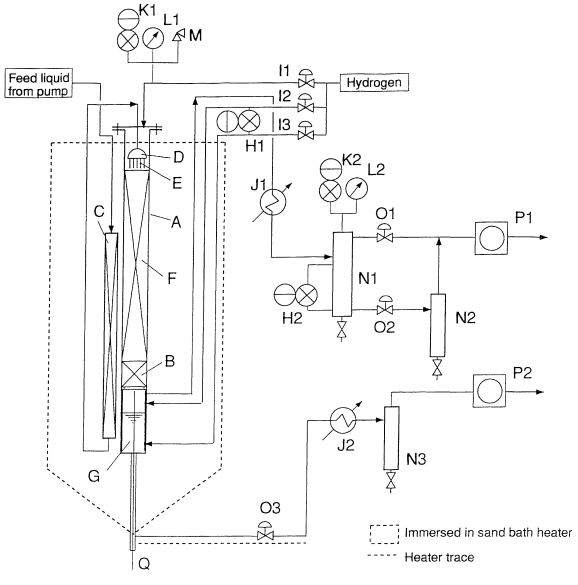

Fig. 1. A schematic drawing of a trickle-bed reactor system: (A) reactor tube; (B) catalyst bed; (C) liquid preheater; (D) inlet liquid distributor; (E) capillary tubes; (F) mixing bed; (G) product flash separator; (H1), (H2) differential pressure transducer; (I1), (I2), (I3) mass flow conroller; (J1), (J2) cooler; (K1), (K2) pressure transmitter; (L1), (L2) pressure gauge; (M) safety valve; (N1), (N2), (N3) flash separator; (O1) control valve to control K2; (O2) control valve to control H2; (O3) control valve to control H1; (P1), (P2) gas meter; (Q) thermowell.

The exit stream from the catalyst bed was separated in PFS into vapor and liquid products. The liquid level of PFS was monitored by a differential pressure transducer (H1). A slight amount of hydrogen (1.39×10^{-7} m^3/s) was fed from mass flow controllers ((I2) and (I3)) into pressure transfer lines to prevent the condensation of liquid in these lines. The volume of vapor in PFS was kept at 30×10^{-6} m^3 by controlling the liquid level in PFS by a control valve (O3).

The vapor product drawn from PFS was cooled and again separated in a series of high and low pressure flash separators ((N1) and (N2)) into gaseous and liquid steams. Similarly, the liquid product from PFS was cooled and separated in a flash separator (N3) into the other gaseous and liquid streams. The flow rates of these gaseous and liquid streams were measured. The compositions of these gaseous and liquid streams were analyzed in accordance with a procedure described in Section 2.5. Thus, we determined the flow rate of each component in the vapor and liquid products drawn from PFS.

Catalyst of 35.2 g (84 mm height) was loaded. The void fraction of the bed and the apparent bed density (ρ_B) were 0.389 and 721 kg/m^3, respectively. A thermowell was not inserted into the catalyst bed to prevent maldistribution of liquid around it. The outlet temperature of the catalyst bed was continuously monitored.

2.4.2. Vapor-phase reaction

The vapor-phase reaction was performed with 5.0 g catalyst using a fixed bed tubular reactor of 8.0 mm inner diameter and 0.5 m length.

2.5. Product analysis

The liquid streams from flash separators ((N2) and (N3) in Fig. 1) were sampled and analyzed by a gas chromatograph equipped with a flame ionization detector and a capillary column (PONA Column, Hewlett Packard). A system gas chromatography equipped with thermal conductivity detectors (manufactured by Shimadzu, Japan) was used to analyze hydrogen and light hydrocarbons (C_1–C_5 fractions) in the gaseous products from gas meters ((P1) and (P2) in Fig. 1). No significant amounts of light hydrocarbons

which can be produced from hydrocracking reaction, were observed in any experiments in the vapor- and three-phase conducted in this study.

2.6. Physical properties in the system

The Soave–Redlich–Kwong (SRK) equation of state [10] was applied for the prediction of vapor–liquid equilibria. Binary interaction parameters in the SRK equation were determined from the binary data for hydrogen and *n*-hexadecane, and for hydrogen and 1-methylnaphthalene from [11]. The binary interaction parameter between *n*-hexadecane and hydrogen was applied for those between other normal paraffins and hydrogen.

The density of vapor can be obtained in the course of the solution of the SRK equation of state. The liquid density and viscosity were calculated in accordance with the method of the American Petroleum Institute [12]. The method of Dean et al. [13] was applied to estimate the viscosity of vapor.

Molecular diffusivities (D_j) of the constituents in the reaction system are necessary to estimate mass transfer coefficients. On the assumption that the liquid-phase can be considered as a binary solution, the Wilke–Chang equation [14] was used to predict the diffusion coefficient at infinite dilution, where the association factor was assumed to be unity. D_j was calculated using a mixing rule for ideal binary solutions [15].

3. Results and discussion

3.1. Qualitative observation of the occurrence of vapor-phase reaction

The three-phase reaction was conducted using TBR at 583 K, 8.0 MPa and 860 gas to feed oil ratio (the volumetric ratio of hydrogen feed rate at the normal state to liquid feed rate at 288 K). Three experimental runs were performed in these conditions at 5.94, 11.78 and 24.9 h^{-1} liquid hourly space velocities (LHSV) by changing the rates of the feed liquid and hydrogen. Over the catalyst used in this study, 1-MN is consecutively hydrogenated to all isomers of methyltetralins (MT) and methyldecalins (MD) as illustrated in Fig. 2 [7,8].

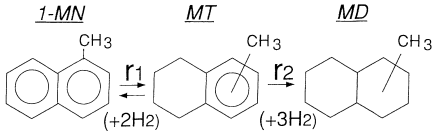

Fig. 2. Reaction path for hydrogenation of 1-MN.

As described in the previous chapter, we can assume the vapor–liquid equilibrium (VLE) at the inlet of catalyst bed because the liquid feed sufficiently contacted hydrogen in the mixing bed. Superficial mass velocities of vapor and liquid at the inlet of catalyst bed for the three runs were calculated assuming VLE and shown in Table 2. As can be seen in Table 2, the liquid superficial mass velocities are low in the reaction conditions. From the calculation of VLE, the vaporized fractions of 1-MN and NPL at the inlet of the catalyst bed were estimated to be 58% and 46%, respectively. The reaction system was highly volatile. Calculated physical properties and mass transfer coefficients are also summarized in Table 2. Gas-to-liquid volumetric mass transfer coefficients, $(ka)_{GL,j}$, and liquid-to-solid volumetric mass transfer coefficients, $(ka)_{LS,j}$, were calculated using Goto and Smith correlations [16]. These coefficients are applied to the simulation of the product distribution of TBR in the latter part of this chapter.

The mass transfer in the mixing bed was simulated using the correlation of $(ka)_{GL,j}$ by Goto and Smith [16]. The results of the simulation supported the assumption of VLE at the inlet of catalyst bed in the three runs.

Fig. 3 shows the plot of yields of MT and MD vs. LHSV (or superficial liquid mass velocity) for the three runs. Temperature at the outlet of the catalyst bed was continuously monitored during the reaction. The deviation of this temperature from the sand bath temperature was within 5 K. The solid and dashed lines in Fig. 3 are calculated results which will be discussed in the later part of this chapter.

In Fig. 4, the ratios of the flow rate of each component in the vapor product from PFS to that in VLE are plotted vs. LHSV (or superficial liquid mass velocity). The ratios for NPL for all the runs were close to unity, i.e. in VLE, which supports the validity of the prediction of vapor–liquid equilibria performed in this study. At the lowest LHSV, the rate of 1-MN in the vapor product from PFS was lower than that in VLE. In this condition, 1-MN in the liquid-phase may

Table 2
Vapor and liquid mass velocities, physical properties, and mass transfer coefficients at the inlet of catalyst bed calculated by assuming the vapor–liquid equilibrium (T=583 K; P=8.0 MPa; 860 gas to oil ratio)

	Run-1	Run-2	Run-3
Liquid hourly space velocity[a] (h^{-1})	5.94	11.78	24.90
Superficial mass velocity[b] ($kg/m^2/s$)			
Vapor-phase	0.061	0.121	0.256
Liquid-phase	0.057	0.113	0.240
Density (kg/m^3)			
Vapor-phase		17.4	
Liquid-phase		550.3	
Viscosity (Pa s)			
Vapor-phase		1.95×10^{-5}	
Liquid-phase		1.47×10^{-4}	
Molecular diffusivity (m^2/s)			
Hydrogen		1.21×10^{-7}	
1-MN		2.63×10^{-8}	
$(ka)_{GL}$ from Goto and Smith [16] (l/s)			
Hydrogen	1.87×10^{-2}	2.47×10^{-2}	3.45×10^{-2}
1-MN	8.69×10^{-3}	1.14×10^{-2}	1.61×10^{-2}
$(ka)_{LS}$ from Goto and Smith [16] (l/s)			
Hydrogen	0.150	0.220	0.347
1-MN	0.0541	0.0786	0.125

[a]Based on liquid feed rate at 288 K.
[b]Based on actual flow rates of vapor and liquid in the vapor–liquid equilibrium.

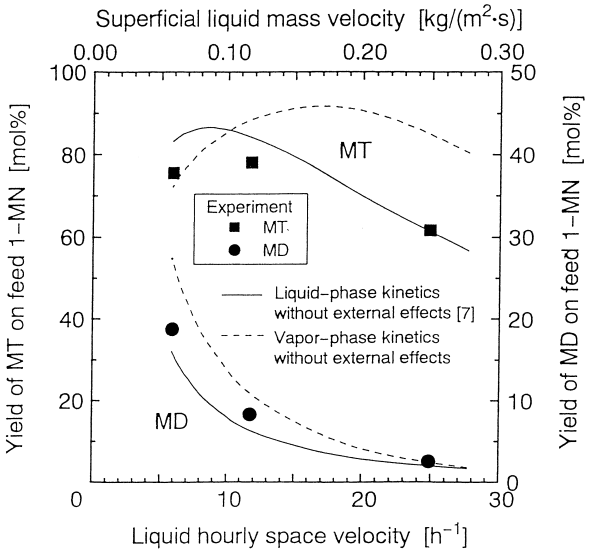

Fig. 3. Yields of MT and MD in TBR and comparison with calculated yields using apparent liquid- or vapor-phase kinetics without external effects.

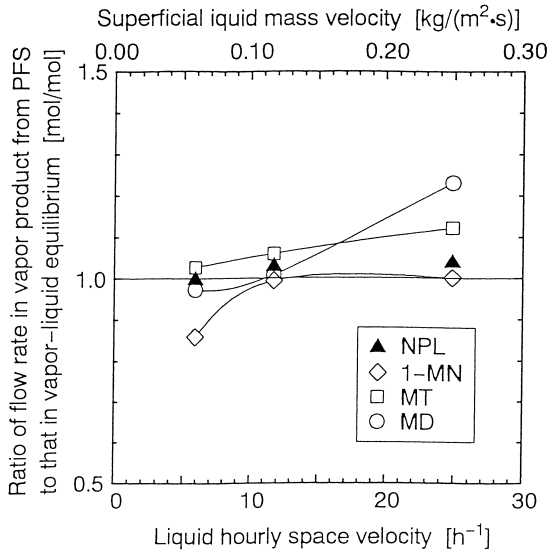

Fig. 4. Plots of the ratios of the flow rate of each component in the vapor product from PFS to that in the vapor–liquid equilibrium.

be consumed more slowly than that in the vapor-phase due to the poor external wetting and the substantial mass transfer limitation. On the other hand, at the highest LHSV, the rate of MT and MD in the vapor product from PFS exceeded those in VLE. This suggests that MT and MD were produced by the direct contact between the reactants in the vapor-phase and dry solid catalyst, and may still remain in the vapor-phase. It was verified that the vapor-phase contributed to the global reaction rate even in the present slow reaction system when the liquid velocity was low and the volatility of the system was high.

To perform the quantitative analysis on the contribution of VPR to the global reaction rate, kinetics in the vapor-phase are necessary. Therefore, the kinetic study on the vapor-phase reaction was conducted in Section 3.2.

3.2. Kinetic study on the vapor-phase reaction

The vapor-phase reaction (VPR) was performed in the range of 583–623 K temperature and 5.0–8.0 MPa total pressure with feed gases of various compositions (Feed-A, -B and -C in Table 1). Data plotted with open symbols in Fig. 5 show the influence of feed gas composition on the yield of MT and MD with the powdered catalyst at 603 K and 5.0 MPa. The highest reaction rate was observed with Feed-C which contained the least 1-MN in the feed gas. This suggests the inhibition of 1-MN and/or hydrogenated product in the vapor-phase reaction.

The influence of pressure at 603 K with Feed-A, and that of temperature at 8.0 MPa with Feed-B on the yield of MT and MD, are shown in Figs. 6 and 7,

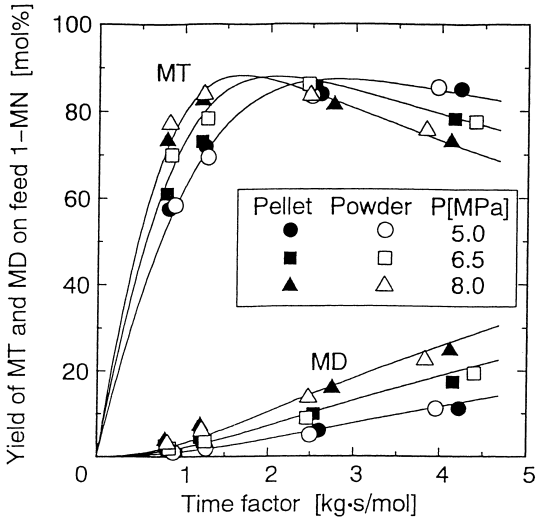

Fig. 6. Influence of pressure on yields of MT and MD with Feed-A in the vapor-phase reaction. All lines: calculated by Eqs. (3), (4), (5)–(10). T=603 K.

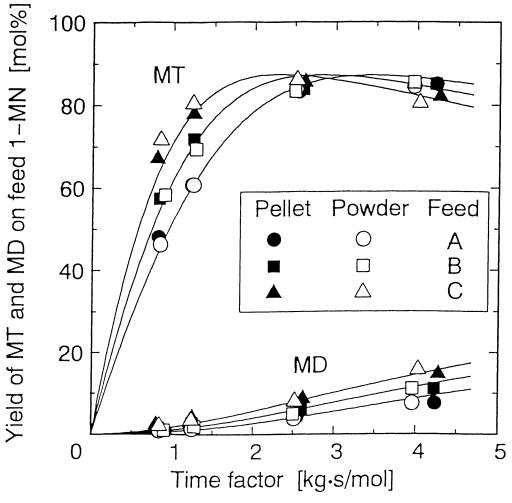

Fig. 5. Influence of feed gas composition on yields of MT and MD in the vapor-phase reaction. All lines: calculated by Eqs. (3), (4), (5)–(10). T=603 K; P=5.0 MPa.

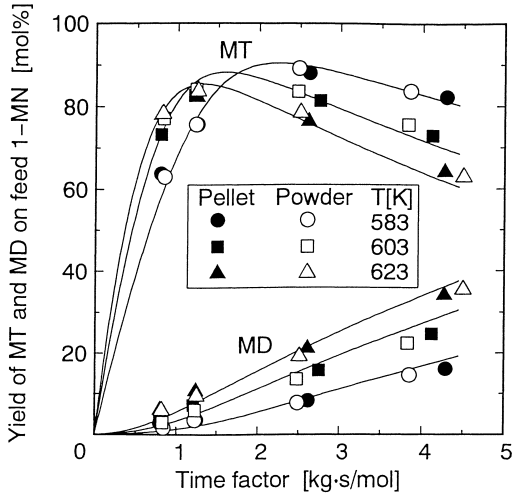

Fig. 7. Influence of temperature on yields of MT and MD with Feed-B in the vapor-phase reaction. All lines: calculated by Eqs. (3), (4), (5)–(10). P=8.0 MPa.

respectively, for the powdered catalyst with open symbols. The increases of temperature and/or pressure accelerated the rate of reaction. In Figs. 5, 6, 7, the results with the pelletized catalyst are also plotted with closed symbols. One can see that all the results with the pelletized catalyst are nearly the same as those obtained with the powdered catalyst even in the conditions where the reaction would proceed at the maximum rate: 623 K, 8.0 MPa with Feed-B as found in Fig. 7. This suggests that the intraparticle diffusion resistances can be ignored for the vapor-phase reaction in the reaction conditions employed in this study.

As a result of the least squares estimation for the kinetic data for VPR, the following Langmuir–Hinshelwood type kinetic equations based on the weight of catalyst (r_1 and r_2) were determined to give the best fit to the results.

$$r_1 = k_1 K_{MN} K_H^2 (P_{MN} P_H^2 - P_{MT}/K_{P1}) \Big/ \left\{ (1 + K_{MN} P_{MN} + K_{MT} P_{MT})(1 + K_H P_H)^2 \right\}., \quad (3)$$

$$r_2 = k_2 K_{MT} K_H^3 P_{MT} P_H^3 \Big/ \left\{ (1 + K_{MN} P_{MN} + K_{MT} P_{MT}) \times (1 + K_H P_H)^3 \right\}.. \quad (4)$$

The equilibrium constant for the primary hydrogenation reaction (K_{P1}) was correlated as a function of temperature using measurements by Bouchy et al. [17]:

$$K_{P1} = \exp(-51.7 + 14600/T). \quad (5)$$

Other parameters (reaction rate constants, k_1, k_2 and adsorption constants, K_{MT}, K_{MN} and K_H) were correlated by the following:

$$k_1 = \exp(16.0 - 11900/T), \quad (6)$$

$$k_2 = \exp(22.3 - 16800/T), \quad (7)$$

$$K_{MN} = \exp(-32.3 + 13400/T), \quad (8)$$

$$K_{MT} = \exp(-33.7 + 13400/T), \quad (9)$$

$$K_H = \exp(-21.6 + 4210/T). \quad (10)$$

Similar values of adsorption constants for one- and two-rings aromatics were presented by Korre and Klein [18] in the vapor-phase hydrogenation of polynuclear aromatic hydrocarbons. Eqs. (3) and (4) suggest that surface reaction between hydrogen and aromatic hydrocarbons on dual adsorption sites, may be rate-limiting. Calculated results using Eqs. (3)–(10) are drawn with solid lines in Figs. 5–7. The intrinsic kinetic model determined for the vapor-phase represented well the influence of feed gas composition, pressure and temperature on the yield of products.

3.3. Simulation of product yields in trickle-bed reactor

3.3.1. Comparison with liquid- or vapor-phase reaction without external effects

The product yields in the reaction with TBR were compared with those calculated using the liquid-or vapor-phase kinetics without external effects. In these calculations, plug-flow and the VLE in the bulk-phase were assumed.

The solid and dashed lines in Fig. 3 show the calculated results using previously reported liquid-phase kinetics [7] and using the vapor-phase kinetics determined in this study, respectively.

The experimental yields of the final product (MD) lie between the two lines. The contribution of VPR would enhance the global reaction rate, especially at the lowest superficial liquid mass velocity.

3.3.2. Conventional partial wetting model assuming complete internal wetting

The product distributions in TBR were also simulated using the conventional partial wetting model [1–3] where the effects of f_w, $(ka)_{GL,j}$ and $(ka)_{LS,j}$ were considered. In this case, the liquid-phase reaction only affects the global reaction rate as expressed in Eq. (1) because one assumes the complete internal wetting of catalyst. A dashed line in Fig. 8 indicates f_w estimated by a correlation of Mills and Dudukovic [19]. In Fig. 9, simulated yields of MT and MD are drawn with dashed lines. Experimental yields of MD were higher than the simulated results.

The experimental yields of MD, especially at the lowest liquid velocity, could not be explained by liquid-, vapor-phase kinetics without external effects, nor the conventional partial wetting model.

3.3.3. Partial wetting model with vapor-phase reaction in completely dry particles

To explain the product yields in TBR, we assumed that the catalyst bed may be composed of externally

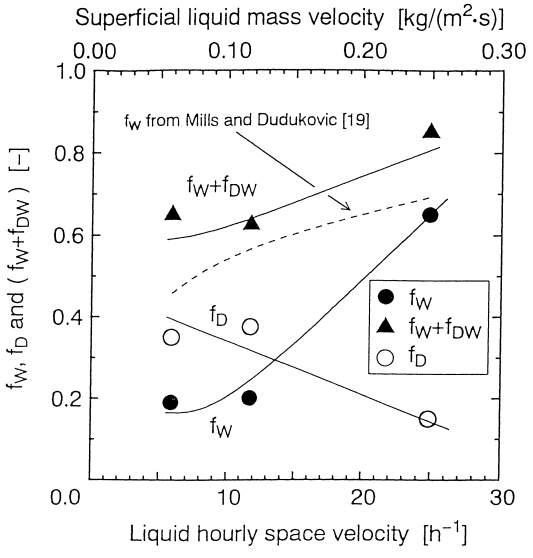

Fig. 8. Plot of f_w, f_D and (f_w+f_{DW}) determined in this study, and f_w calculated by the correlation of Mills and Dudukovic [19].

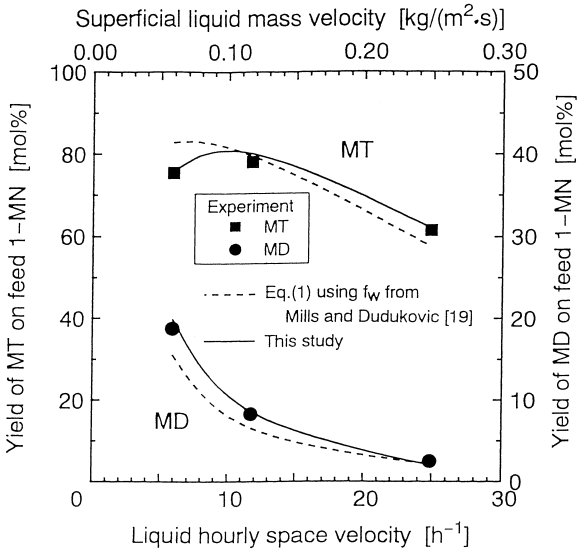

Fig. 9. Comparison of calculated yields of MT and MD in TBR using two models. Solid lines: partial wetting model with vapor-phase reaction in completely dry catalyst presented in this study. Dashed lines: partial wetting model in Eq. (1) using f_w by the correlation of Mills and Dudukovic [19].

partial and internally complete wet particles, and completely dry particles as illustrated in Fig. 10. The fractions of wetted and non-wetted regions in the wetted particles are defined as f_W and f_{DW}, respectively. Completely dry particles (fraction f_D) may appear as a result of the vaporization of volatile liquid components induced by poor heat transfer at the gas–solid interface in highly exothermic reactions. In this assumption, the global reaction rate can be expressed as:

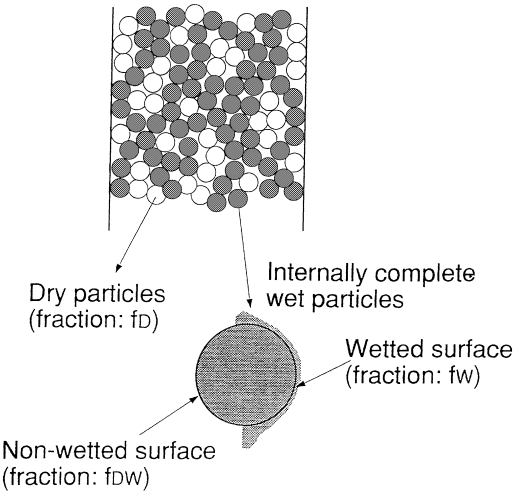

Fig. 10. Trickle-bed assumed in this study: the bed composed of externally partial and internally complete wet particles, and dry particles.

$$r'_{GL,j} = f_W r'_{L,j}(C_L) + f_{DW} r'_{L,j}(C^*_L) + f_D r'_{G,j}(C^*_G), \quad (11)$$

where gas-to-solid mass transfer resistances were assumed to be negligibly small. Hence, mass balances between the liquid- and vapor-phases can be expressed as the following equations:

$$d(u_L C_{L,j})/dz = (ka)_{GL,j}(C^*_{L,j} - C_{L,j}) - (ka)_{LS,j}(C_{L,j} - C_{S,j}), \quad (12)$$

$$d(u_G C_{G,j})/dz = -(ka)_{GL,j}(C^*_{L,j} - C_{L,j}) - f_{DW}\rho_B r'_{L,j}(C^*_L) - f_D \rho_B r'_{G,j}(C^*_G), \quad (13)$$

where

$$(ka)_{LS,j}(C_{L,j} - C_{S,j}) = f_W r'_{L,j}(C_S), \quad (14)$$

$$f_W + f_{DW} + f_D = 1, \quad (15)$$

and

$$C_{L,j} = C^*_{L,j} \quad \text{and} \quad C_{G,j} = C^*_{G,j} \quad \text{at } z = 0. \quad (16)$$

Using this model, the values of f_D and f_w were determined to explain the yields of MT and MD in TBR. The determined values of f_W and f_D and calculated yields of MT and MD are shown in Figs. 8 and 9, respectively. This model suitably explained the yields of MT and MD. With the increase of liquid velocity, f_W increases from 0.20 to 0.62, and f_D decreased from 0.38 to 0.15.

In Fig. 8, the sums of f_W and f_{DW} which correspond to the fraction of externally partial and internally complete wet particles in this model, are also plotted. The values of f_W+f_{DW} were similar to f_W estimated by the correlation of Mills and Dudukovic [19]. This suggests that the catalyst particles which can be completely wetted in a non-volatile reaction system may turn into the partially wet particles during the exothermic reaction performed at low liquid velocities in the presence of highly volatile liquid-phase components.

4. Conclusion

In the hydrogenation of 1-MN performed using a laboratory-scale trickle-bed reactor, it was qualitatively confirmed that the vapor-phase reaction contributed to the global three-phase reaction rate in this slow exothermic reaction when the liquid velocity is low and the volatility of the system was high.

To perform the quantitative analysis on the contribution of vapor-phase reaction to the global reaction rate, Langmuir–Hinshelwood type kinetic equations for the vapor-phase reaction were established.

The experimental data in the trickle-bed reactor could not be explained by liquid-, vapor-phase kinetics without external effects, nor the conventional partial wetting model.

A partial wetting model considering the contribution of the vapor-phase reaction was proposed where the catalyst bed composed of externally partial and internally complete wet particles, and completely dry particles was assumed. Using this model, the product yields in the trickle-bed reactor were suitably explained. The existence of 15–38% completely dry particles was suggested in the range 0.057–0.240 kg/(m^2 s) superficial liquid mass velocity.

The presented model may be applied to analyze the performance of trickle-bed reactors operated at low liquid velocities under highly volatile conditions for highly exothermic and volatile reaction system.

5. Nomenclature

C_i	concentrations in phase-i (mol/m^3)
$C_{i,j}$	concentration of component-j in phase-i (mol/m^3)
C_i^*	concentrations of phase-i in the vapor–liquid equilibrium (mol/m^3)
C_{ij}^*	concentrations of component-j in phase-i in the vapor–liquid equilibrium (mol/m^3)
f_D	fraction of completely dry particles (dimensionless)
f_{DW}	fraction of externally non-wetted and internally wet surface (dimensionless)
f_W	fraction of externally and internally wet particles (dimensionless)
$(ka)_{GL,j}$	volumetric gas-to-liquid mass transfer coefficient of component-j (l/s)
$(ka)_{LS,j}$	volumetric liquid-to-solid mass transfer coefficient of component-j (l/s)
K_{P1}	equilibrium constant in the vapor-phase for the first reaction in Fig. 2 (Pa^2)
K_j	adsorption constant of component-j in the vapor-phase (m^3/mol)
k_1	reaction rate constant for r_1 in Fig. 2 (mol/(s kg-cat))
k_2	reaction rate constant for r_2 in Fig. 2 (mol/(s kg-cat))
P	total pressure (Pa)
P_j	partial pressure of component-j (Pa)
r_1	reaction rate in the vapor-phase for the first reaction to produce 1-methylnaphthalene to methyltetralins (mol/(s kg-cat))
r_2	reaction rate in the vapor-phase for the second reaction to produce methyltetralins to methyldecalins (mol/(s kg-cat))
$r'_{G,j}$	apparent vapor-phase reaction of component-j (mol/(s kg-cat))
$r'_{GL,j}$	global three-phase reaction rate of component-j (mol/(s kg-cat))
$r'_{L,j}$	apparent liquid-phase reaction rate of component-j (mol/(s kg-cat))
T	temperature (K)
u_i	superficial velocity of phase-i (m/s)
z	reactor length (m)

ρ_B catalyst bed density (kg/m^3)

Subscripts

i	phase-*i*
j	component-*j*
H	hydrogen
1-MN	1-methylnaphthalene
MT	methytetralins
MD	methyldecalins
G	vapor-phase
L	liquid-phase
S	solid surface
PFS	product flash separator

References

[1] A.J. Colombo, G. Baldi, S. Scardi, Chem. Eng. Sci. 31 (1976) 1101.
[2] S. Goto, A. Lakota, J. Levec, Chem. Eng. Sci. 36 (1981) 157.
[3] C.N. Satterfield, F. Ozel, AIChE J. 19 (1973) 1259.
[4] W. Sedriks, C.N. Kenney, Chem. Eng. Sci. 28 (1973) 559.
[5] T.-C. Huang, B.-C. Kang, Ind. Eng. Chem. Res. 34 (1995) 2349.
[6] C.M. Ruecker, A. Akgerman, Ind. Eng. Chem. Res. 26 (1987) 164.
[7] S. Ishigaki, S. Goto, J. Chem. Eng. Jpn. 27 (1994) 309.
[8] S. Ishigaki, S. Goto, J. Chem. Eng. Jpn. 28 (1995) 329.
[9] S. Ishigaki, S. Goto, J. Chem. Eng. Jpn. 30 (1997) 64.
[10] G. Soave, Chem. Eng. Sci. 27 (1972) 1197.
[11] C.L. Young, Solubility Data Series, vol. 5/6, Pergamon Press, Oxford, 1981, pp. 373 and 428.
[12] American Petroleum Institute, Technical Data Book: Petroleum Refining, 5th ed., API, USA, 1991, p. 65.
[13] D.G. Dean, L.S. Stiel, AIChE J. 11 (1965) 526.
[14] C.R. Wilke, P. Chang, AIChE J. 1 (1955) 264.
[15] A. Vignes, Ind. Eng. Chem. Fundam. 5 (1966) 189.
[16] S. Goto, J.M. Smith, AIChE J. 21 (1975) 706.
[17] M. Bouchy, S.P. Denys, P. Dufresne, S. Kasztelan, Ind. Eng. Chem. Res. 32 (1993) 1592.
[18] S.C. Korre, M.T. Klein, Ind. Eng. Chem. Res. 34 (1995) 101.
[19] P.L. Mills, M.P. Dudukovic, AIChE J. 27 (1981) 893.